Biosensors and Bioelectronics 99 (2018) 555–563

Contents lists available at ScienceDirect

Biosensors and Bioelectronics

journal homepage: www.elsevier.com/locate/bios

A novel and simple cell-based electrochemical biosensor for evaluating the antioxidant capacity of *Lactobacillus plantarum* strains isolated from Chinese dry-cured ham

Qingfeng Ge[a,b], Panwei Ge[b], Donglei Jiang[b,d], Nan Du[b], Jiahui Chen[b], Limin Yuan[c], Hai Yu[b], Xin Xu[b], Mangang Wu[b], Wangang Zhang[a,*], Guanghong Zhou[a]

[a] *Key Laboratory of Meat Processing and Quality Control, MOE, Key Laboratory of Meat Processing, MOA, Jiangsu Synergetic Innovation Center of Meat Processing and Quality Control, College of Food Science and Technology, Nanjing Agricultural University, Nanjing 210095, PR China*

[b] *School of Food Science and Technology, Yangzhou University, Industrial Engineering Center for Huaiyang Cuisin of Jiangsu Province, Yangzhou, Jiangsu 225127, PR China*

[c] *Testing Center, Yangzhou University, Yangzhou, Jiangsu 225009, China*

[d] *Jiangsu key Laboratory of Zoonoses, Yangzhou, Jiangsu 225009, China*

ARTICLE INFO

Keywords:
Antioxidant capacity
RAW264.7 cells
Lactobacillus plantarum strains
Hydrogen peroxide
Electrochemical assay

ABSTRACT

The analysis of antioxidants in foodstuffs has become an active area of research, leading to the recent development of numerous methods for assessing antioxidant capacity. Here we described the fabrication and validation of a novel and simple cell-based electrochemical biosensor for this purpose. The biosensor is used to assess the antioxidant capacity of cell-free extracts from *Lactobacillus plantarum* strains isolated from Chinese dry-cured ham. The biosensor relies on the determination of cellular reactive oxygen species (ROS) (the flux of H_2O_2 released from RAW 264.7 macrophage cells) to indirectly assess changes in intracellular oxidative stress level as influenced by *L. plantarum* strains. A one-step acidified manganese dioxide (a-MnO_2) modified gold electrode (GE) was used to immobilize RAW 264.7 macrophage cells, which were then encapsulated in a 3D cell culture system consisting of alginate/ graphene oxide (NaAlg/GO). The biosensor exhibited a rapid and sensitive response for the detection of H_2O_2 released from RAW264.7 cells. The detection limit was 0.02 μM with a linear response from 0.05 μM to 0.85 μM and the biosensor was shown to have good stability and outstanding repeatability. This technique was then used for evaluating the antioxidant ability of extracts from *L. plantarum* NJAU-01. According to the electrochemical investigations and assays of SEM, TEM, and ROS, these cell-free extracts effectively reduced the oxidative stress levels in RAW264.7 cells under external stimulation. Extracts from *L. plantarum* strains at a dose of 10^{10} CFU/mL showed the highest antioxidant activities with a relative antioxidant capacity (RAC) rate of 88.94%. Hence, this work provides a simple and efficient electrochemical biosensing platform based on RAW264.7 cells for fast, sensitive and quantitative assessment of antioxidant capacity of *L. plantarum* strains. The method demonstrates its potential for rapid screening for evaluating antioxidant properties of samples.

1. Introduction

Reactive oxygen species (ROS) are generated naturally *in vivo* during metabolic processes. In normal living organisms ROS is kept in balance as it has important physiological effects on transcription factors, cell proliferation and differentiation (Wang et al., 2014). However, the accumulation of excess ROS in organisms, as a result of a harmful environmental stress, could cause damage to nucleic acids, proteins and lipids, impede normal cellular metabolism, and induce various diseases such as aging, initiate cancer, heart disease and arteriosclerosis (Dickinson and Chang, 2011).

Therefore, overproduction of ROS can be extremely harmful to body health (Pi et al., 2017). Thus, most living organisms have developed enzymatic and non-enzymatic antioxidant defense systems to counteract the deleterious effects of ROS (Ahmad et al., 2017). However, these cellular antioxidative systems are not always able to prevent living organisms from oxidative damage. Hence, exogenous synthetic and natural antioxidants capable of removing free radicals and other pro-oxidants have been largely studied (Blois, 1958). The safety of synthetic antioxidants has recently been questioned due to their potential hepatotoxicity and carcinogenicity (Luo and Fang,

* Corresponding author.
E-mail address: wangang.zhang@njau.edu.cn (W. Zhang).

http://dx.doi.org/10.1016/j.bios.2017.08.037
Received 5 June 2017; Received in revised form 11 August 2017; Accepted 14 August 2017
Available online 15 August 2017

2008). Therefore, as a safer alternative, extracts from mixed *Lactobacillus plantarum* strains isolated from traditional Chinese dry-cured ham, have recently received much attention for their *in vitro* scavenging activity against hydroxyl and 2,2-diphenyl-1-picryl-hydrazyl (DPPH) free radicals, and for their resistance to hydrogen peroxide (Li et al., 2012).

Many methods have been devoted to evaluating antioxidant activity in the area of food technology, including photometric (Pazourek et al., 2005; Prenesti et al., 2007), fluorimetric (Ou et al., 2001; Qiao et al., 2015), chromatography (Gimeno et al., 2015) and electrochemical methods (Gao et al., 2015; Ignatov et al., 2002; Kamel et al., 2008; Reybier et al., 2010; Wang et al., 2015). Among these methods, the electrochemical strategy has been used for assessing antioxidant capacities because of its high sensitivity, fast response time, simple operation, low cost and accuracy (Andlauer and Heritier, 2011; Bordonaba and Terry, 2012; Cata et al., 2016; Chakraborty and Raj, 2009; Romero et al., 2017). In particular, the differential pulse voltammetry (DPV) technique is suitable for rapid real-time monitoring as it has high temporal resolution properties as well as good dynamic kinetic characteristics for electrochemical redox process (Ervin and Kariuki, 2014; Tufan et al., 2014; Zhang et al., 2015; Zhao et al., 2017). However, most of these electrochemical studies have focused on the modification of electrodes for detecting radical scavengers or for DNA damage, while methods based on living cells for the determination and the evaluation of antioxidant activity have not been reported. Therefore, the exploitation of an actual or more realistic technique for antioxidant measurement has become important.

Recently, cell-based biosensors have been widely used in many fields, including drug screening, environmental testing, medical diagnosis, and national security (Jiang et al., 2014). Using the natural ability of macrophage cells to detect and determine oxidative stress provides a stable and accurate strategy mimicking physiological conditions. For instance when RAW264.7 cells are activated with phorbol 12-myristate 13-acetate (PMA) within a short time, it triggers the generation of ROS in the cytoplasm causing the release of H_2O_2 (Wang et al., 2016). Hence, RAW 264.7 cells have an excellent potential for the application of electrochemical biosensors as a result of their sensitivity to high oxidative stress. The cells can be used to evaluate the antioxidant activity of specific antioxidants and convert biological recognition into a signal that can be readily recorded and quantified (Rider et al., 2003). The H_2O_2 from RAW264.7 cells which is immobilized on an electrode can be detected rapidly and accurately converted to a sensitive and specific electrochemical signal.

For producing cell-based electrochemical biosensors, the immobilization of cells on an appropriate transducer surface is a crucial step in the electrochemical process, in order to achieve the signal sensitively, stably and reproducibly (Taniguchi, 2010). To achieve optimal cell adhesion and to maintain cell viability, alginate (NaAlg) and Graphene oxide (GO) hydrogels can be used to encapsulate RAW264.7 cells and provide a three dimensional (3D) culture system for maintaining cell activity as well as preventing environmental interference (Lee et al., 2016). This technique provides excellent biocompatibility and electrical conductivity and hydrophilicity, and has strong mechanical strength.

The recent fast development of nano-science and nano-technology has played an important role in improving electro-analytical performance leading to their excellent electrical conductivity, large specific surface areas and biocompatibilities (Zhao et al., 2017). Because of the excellent catalytic oxidation properties, nano-materials have been widely used as catalysts and electrode materials for ROS species detection (Feng et al., 2016). However, the complex fabrication step and the mechanism of action are always the shortcomings of these MnO_2 nano-particle-based sensors. Hence, a one-step modification has become essential for fast detection. Recently, acidified MnO_2 (a-MnO_2) has attracted much attention due to its easier method of synthesis, improved catalytic properties and lower charge-transfer resistance, making it become an excellent modified material for the detection of H_2O_2 released from living cells (Bai et al., 2017). Thus, with the assistance of these nano and biocompatible materials, the 3D cell culture systems developed for evaluating antioxidant capacity have achieved fast, direct electron transfer between immobilized macrophage cells and the fabricated electrode surface, resulting in improved sensitivity and selectivity (Das et al., 2016).

In this study, a simple and novel electrochemical RAW264.7 cell-based sensor was explored for the electrochemical assessment of the antioxidant capacities of extracts from *L. plantarum*. The synthesis of A-MnO_2 was achieved using a mixture of sulfuric acid and nitric acid and was modified on GE by physical adsorption. The NaAlg/GO hydrogel was prepared for the capsulation of RAW264.7 in order to create an *in vitro* 3D culture system. The encapsulation of the living cell, mimicking culture conditions, is thus unaffected by external interferences, and can extend the actual working life of macrophage cells. Then the a-MnO_2 "one-step" modified gold electrode was used to immobilize RAW264.7 cells capsulated in NaAlg/GO hydrogel. The antioxidant and the redox profile of *L. plantarum* extracts were characterized by various electrochemical responses caused by oxidative stress changes in cells. Biological assays including CCK-8, flow cytometry and ROS were carried out to verify the cell electrochemical results.

2. Experimental procedure

2.1. Materials and apparatus

Graphite was obtained from Xian Feng Nano-materials Technology Co. Ltd (Nanjing, China). MnO_2 was purchased from DK Nano-technology Co. Ltd (Beijing, China).

RAW 264.7 macrophage cells were obtained from the Cell Bank of Chinese Academy of Sciences (Shanghai, China). Phorbol 12-myristate 13-acetate (PMA, ≥99%) and alginate sodium were obtained from Sigma-Aldrich Inc (St. Louis, MO, USA). Dulbecco's Modified Eagle Medium (DMEM) and fetal bovine serum were obtained from Gibco Laboratories (Gaithersburg, MD, USA). All cell assay kits were purchased from Beyotime Biotechnology Co. Ltd (Shanghai, China), all solutions were prepared with deionized water and all reagents were of analytical grade.

All electrochemical experiments were performed on a CHI660E electrochemical workstation (Chenhua Technology Co., Ltd., Shanghai, China) using a conventional three-electrode system in a solution containing 1.0 mM of $Fe(CN)_6^{3-/4-}$ or in 0.1 M PBS solution (pH 7.4). The structure of nano-materials and the morphologies of cells were characterized using a transmission electron microscope (Tecnai 12, Philips, Netherlands) and a scanning electron microscope (S-4800 II, Hitachi, Japan). The FT-IR spectrum was recorded on a Fourier transform infrared (FT-IR) spectrometer (FI-IR, NICOLET MEXUS 470, Thermo Electron Corporation, Ramsey, Minnesota, USA) using a KBr disk at a resolution of 4 cm^{-1}. RAW264.7 cells were incubated in a CO_2 incubator (Thermo Scientific Forma Series II Water Jacket, Thermo Fisher Scientific Inc., Rockford, Illinois, USA).

2.2. Preparation of cell-free extracts of Lactobacillus plantarum strains

Lactobacillus plantarum NJAU-01, previously isolated from traditional Chinese dry-cured ham, was used for the inoculation of fermented sausage as starter cultures. It was identified by API 50 CHL kit (BioMérieux Inc., France) and 16S rDNA sequencing analysis. The strains were grown in MRS broth at 37 °C for 18 h.

The intracellular cell-free extracts were prepared by the method of Li et al. (2012) with minor modifications. Firstly, the bacterial cells were harvested, washed and resuspended in de-ionized water. The bacterial numbers were adjusted to 10^5, 10^6 10^7, 10^8, 10^9 and 10^{10} CFU/mL. For each dilution, the cells were incubated with 1 mg/

mL lysozyme at 37 ℃ for 30 min followed by ultrasonic disruption in an ice bath. After removing the cell debris by centrifugation (8000 g, 10 min, 4 ℃), the resulting supernatants were obtained and termed intracellular cell-free extracts of *L. plantarum* strains. Further physiological and biochemical information of *L. plantarum* is given in Supplementary material Fig. S1 and Table S1.

2.3. Preparation of the acidified MnO_2 nano-particles

The a-MnO_2 was prepared from purified MnO_2 using the method of Bai with some modification (Bai et al., 2017). Briefly, 50 mg MnO_2 were dissolved in mixture of concentrated H_2SO_4 and HNO_3 (3:1, v/v ratio) in an ultrasonic bath. Then, the mixture was stirred for 4 h in an ice bath. After centrifugation, washing and drying, the a-MnO_2 was obtained. The preparation method for the modified electrode was as follows: 1 mg a-MnO_2 nano-materials was dispersed in chitosan solution (1 mL, 1 mg/mL) using ultrasound. Then 10 μL suspension was dropped on the surface of a dry gold electrode (GE). The modified electrode is defined as a-MnO_2/GE.

2.4. RAW264.7 cell culture

RAW 264.7 macrophage cells were cultivated in Dulbecco's Modified Eagle Medium (DMEM) supplemented with 10% (v/v) fetal bovine serum. The cells were maintained at 37℃in a 5% CO_2 environment. After growing to 90% confluence, the cells were then washed three times with PBS and the cell number was estimated by a hemocytometer (Wu et al., 2011).

2.5. Construction of the cell-based sensor

In order to immobilize the RAW264.7 cells on the a-MnO_2/GE for the construction of the cell-based sensor, the following steps were used. Firstly, NaAlg/ GO hydrogels were prepared as described previously (Jiang et al., 2017). Characterization of the GO and GO/NaAlg hydrogel is shown in Supplementary material Fig. S4. Then, for encapsulating the RAW264.7 cells in the NaAlg/GO hydrogels in a 3D culture system, RAW264.7 cells in the logarithmic phase of growth of were collected, counted and washed. About 5×10^7 viable cells/mL was suspended in complete serum-free medium. Then 1 mL cell suspension was gently mixed with 1 mL NaAlg/GO hydrogel and stored at 37 °C for 5 min. After that, 5 μL cell/ NaAlg/GO suspension was dropped onto the surface of a-MnO_2/GE and then the GE was immersed into a tube containing 100 mM $CaCl_2$-buffered DMEM culture medium and left for 5 min at 37 °C to achieve cell immobilization for subsequent electrochemical measurements.

2.6. Cell-based sensor for determination of antioxidant capacity

Electrochemical experiments for antioxidant measurements were performed using a CHI660E electrochemical workstation with a conventional three-electrode system, comprised of a platinum wire as an auxiliary (CE), a Ag/AgCl electrode as a reference (RE), and a modified Cell/NaAlg/GO/a-MnO_2/GE as a working electrode (WE).

Electrochemical detection of hydrogen peroxide released from cells was achieved by stimulating RAW264.7 cells on the electrode with different concentrations of PMA to induce cells to generate H_2O_2. Firstly, the Cell/NaAlg/GO/a-MnO_2/GE was immersed into serially diluted PMA (ranging from 0 to 100 ng mL^{-1}) in Tyrode's buffer for 10 min at 37 °C. After three washes with PBS (pH 7.4), the Cell/NaAlg/GO/a-MnO_2/GE was then connected to the electrochemical workstation. Next, CV, DPV and EIS signals were recorded in the electrolyte containing 1.0 mM of $Fe(CN)_6^{3-/4-}$ or in 0.1 M PBS solution (pH = 7.4). The CV was scanned within a potential range from −0.2 V to +0.6 V with a scan rate of 100 mV/s. The DPV was recorded in a potential range between −0.4 V and 0.2 V with a pulse amplitude of 0.05 V, a pulse width of 0.05 s and a pulse period of 0.2 s.

The antioxidant capacity of *L. plantarum* was evaluated by the same procedures as above except for mixing the *L. plantarum* extracts with Cell/NaAlg/GO hydrogels before PMA stimulation. RAW264.7 cells without being stimulated with PMA served as the control. All experiments were carried out in a water bath at 37 °C.

2.7. Conventional cell-based assays for antioxidant measurements

Cell apoptosis was evaluated by flow cytometry with an Annexin V-FTIC apoptosis Kit (Beyotime, Haimen, China). Briefly, RAW264.7 cells (5×10^7 cells/mL) were incubated with various concentrations of H_2O_2 for 10 min. After the challenge, cells were collected and washed twice with PBS. Collected cells were suspended and labeled with annexin V-FTIC and propidium iodide (PI) for 15 min at 25 °C in the dark, then analyzed by flow cytometry (FACSAria IIu, BD Bioscience, USA) in Diva Cytometer Software (BD Bioscience, USA). Cells that stained positive for Annexin V were counted as apoptotic.

The intracellular generation of ROS was investigated using 6-carboxy-2, T-dichloro-dihydrofluorescein diacetate and di (acetoxy ester) (DCFH-DA) (Molecular Probes, Eugene, OR). Cells pre-incubated in the presence of 10 μM of DCFH-DA for 1 h were treated with different concentrations of LPS for 3 h. The cells were washed three times with serum-free medium. Fluorescence was observed using a fluorescence microscope (IX2-ILL100, Olympus, Tokyo, Japan) with an excitation of 488 nm and an emission of 525 nm. The fluorescence intensity inside the cells was determined using a fluorescence spectrophotometer (Tecan, M200Pro, Switzerland). In addition, total superoxide dismutase (SOD) and malondialdehyde (MDA) generated in cells were measured with the assay kit according to the manufacturer instructions.

3. Results and discussion

3.1. Working principles of the cell-based sensor

An illustration of the fabrication process and working principle of the RAW264.7 cell-based sensor, in terms of determining and evaluating the antioxidant capacity of extracts of *L. plantarum* strains, is shown in Scheme 1. RAW264.7 cells were successfully encapsulated in NaAlg/GO hydrogel and immobilized on the surface of a-MnO_2 modified GE. The Cell/NaAlg/GO/a-MnO_2/GE was then immersed into a calcium bath to form a 3D hydrogel scaffold that considerably enhanced cell adhesion, retained cell activity and protected cells from electrolyte toxicity or any external disturbance (Jiang et al., 2017). When the RAW264.7 cells were stimulated with MPA (ROS stimulator), it induced the production of H_2O_2 in macrophages by activating protein kinase C (PKC) and triggering respiratory burst (Wu et al., 2011). Then H_2O_2 was released from RAW264.7 cells and was adsorbed by the a-MnO_2/GE and catalyzed at the active sites on the surface of MnO_2. At that point, MnO_2 would be reduced and electro-oxidized at the electrode surface (Eqs. (1) and (2)). It may enhance the redox probe from accessing the electrode surface and accelerate the electron-transfer. As a result, the oxidation current greatly increased with the generation of H_2O_2, while the reduction current only increased slightly (Xu et al., 2010).

STEP1: (1)

$$MnO_2 + H_2O_2 \rightarrow Mn_2O_3 + O_2 + H_2O$$

$$MnO_2 + H_2O_2 \rightarrow Mn(OH)2 + O_2$$

STEP 2: (2)

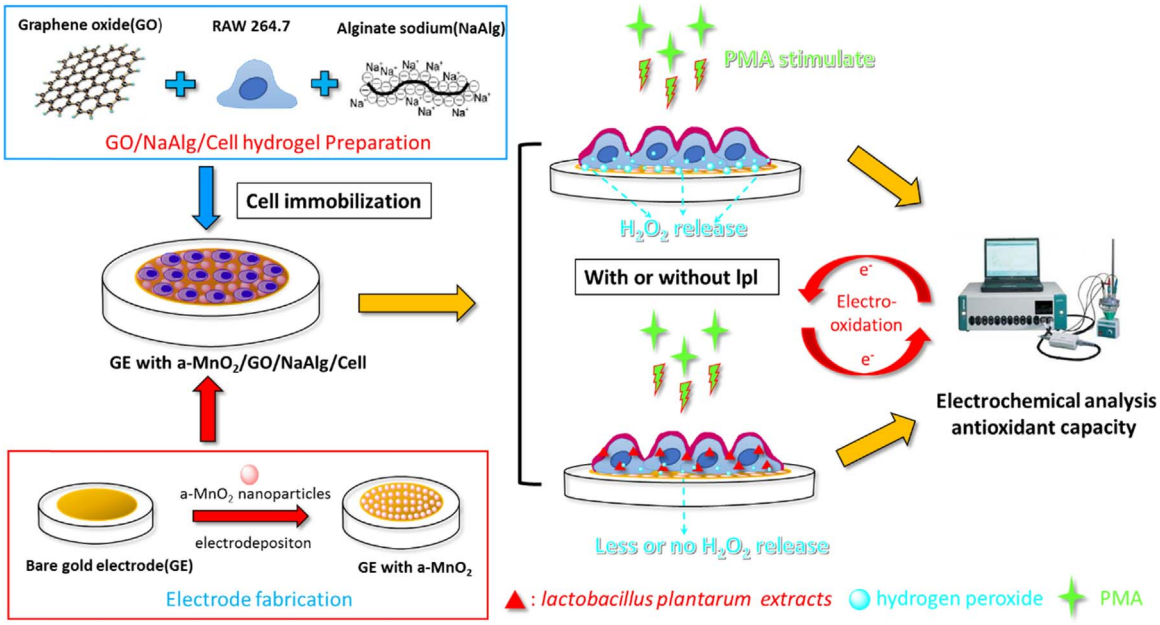

Scheme 1. Schematic illustration for the preparation of RAW264.7 cell-based sensor and process of antioxidant measurements.

$$Mn_2O_3 + 2OH^- \rightarrow 2MnO_2 + H_2O + 2e^-$$

$$Mn(OH)_2 + 2OH^- \rightarrow MnO_2 + 2H_2O + 2e^-$$

When the *L. plantarum* extract was present with the RAW264.7 cells, they would be protected from PMA stimulus and dramatically reduce the occurrence of oxidative stress in cells. With a reduction of H_2O_2 in the cells it reduced the catalytic reaction with MnO_2 and decreased the electron transfer rate of the working electrode, thus resulting in the relative stabilization of the redox current. Hence, through this RAW264.7 cell-based sensor, oxidative stress level in cells

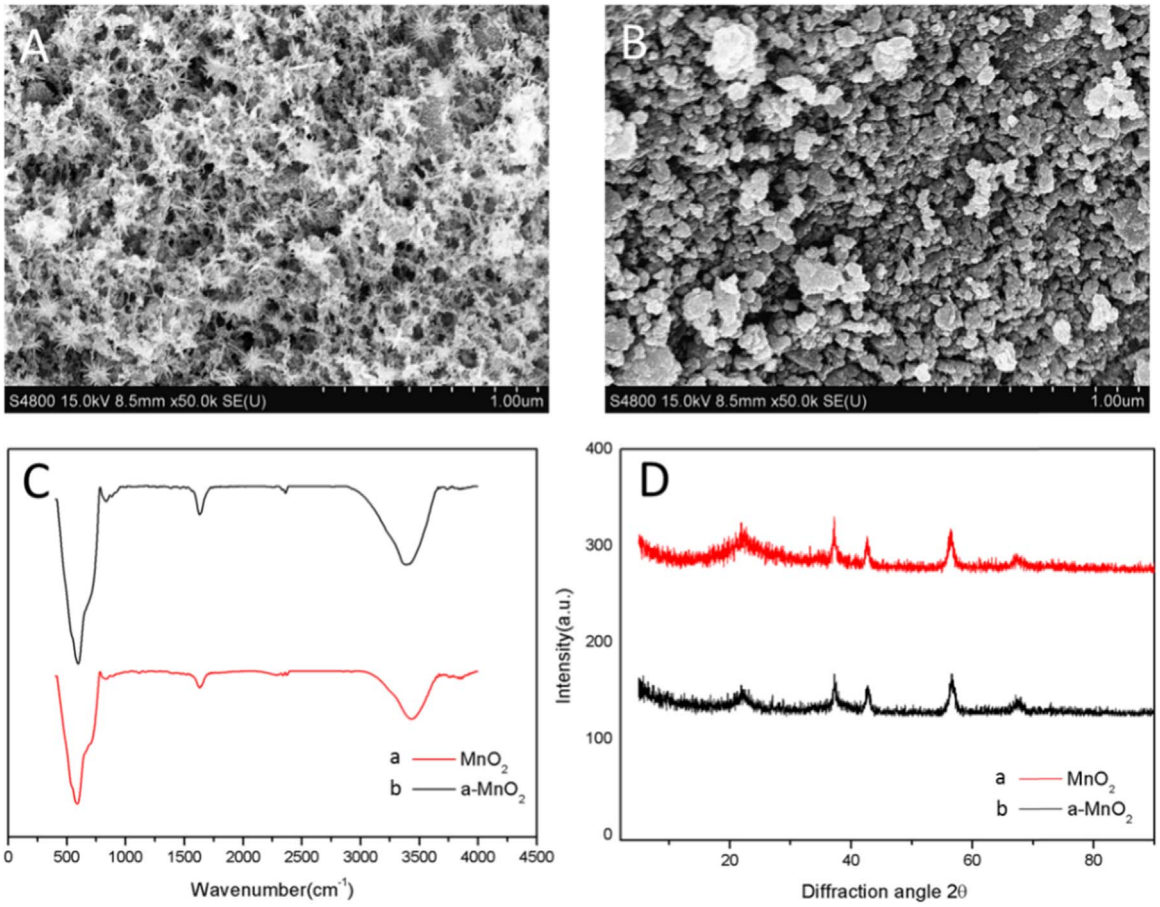

Fig. 1. SEM patterns a-MnO_2 (A) and MnO_2 (B) nanomaterials. FTIR spectra (C) of MnO_2 (a) and a-MnO_2 (b). XRD (D) patterns of MnO_2 (a) and a-MnO_2 (b).

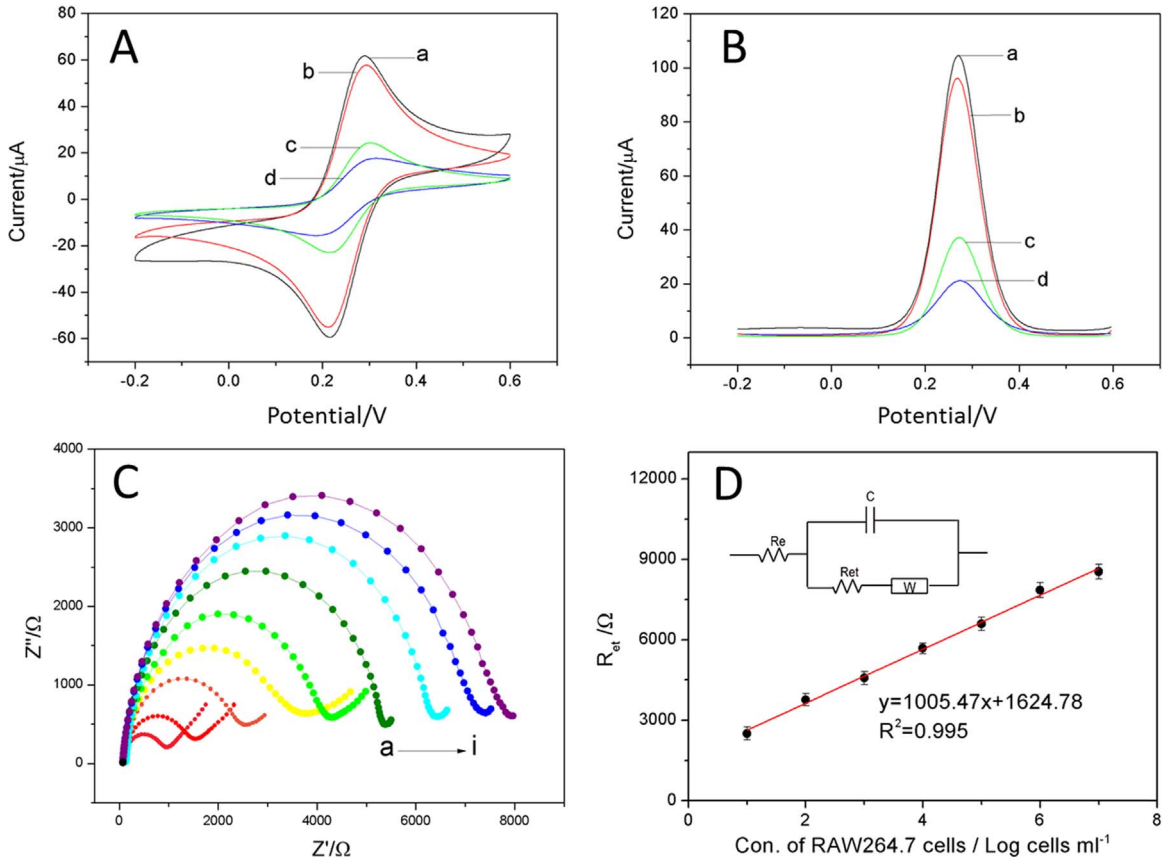

Fig. 2. Electrochemical characterization of the RAW264.7 cell-based sensor. (A) Cyclic voltammograms and (B) Differential pulse voltammetry of (a) bare GE, (b) a-MnO_2/GE, (c) GO/ NaAlg/ a-MnO_2/GE, (d) NaAlg/GO/cell/ a-MnO_2/GE. (C) Nyquist diagrams of (a) bare GE, (a) a-MnO_2/GE (c) to (i): 5 × 10 to 5 × 10^7 cells/mL of RAW246.7 cells immobilized on gold electrode. (D) Linear regression curve between cell concentrations and R_{et} value.

is measured accurately with high sensitivity. This then enables the rapid evaluation of antioxidant capacity of the various extracts of *L. plantarum*.

3.2. Characterization of the nano-materials

Fig. 1A shows the SEM images of MnO_2. As reported previously (Bai et al., 2017), synthetic MnO_2 nano-particles exhibited well-regulated and flower-like structures which comprised of a wrinkle-like nano-layer. However, the morphology of the a-MnO_2 changed markedly after acidification, compared with MnO_2 (Fig. 1B). This may be due to a corrosion effect of concentrated acid on MnO_2 during the preparation process. The reaction proceeded slowly with corrosion of the ball-shaped structure of MnO_2. The diameter of a single flower-like structure was about 100 nm and the monolayer was extremely thin.

Fig. 1C shows the FTIR spectra of materials (Fig. 1C a for MnO_2 and Fig. 1C b for a-MnO_2). The band near 750 cm^{-1} in Fig. 1C is possibly due to the Mn-O stretching vibrations which may be caused by the manganese oxide lattice (MnO_6 octahedral). The 3400 cm^{-1} band can be attributed to the hydroxide group and the peak at 1698 cm^{-1} to the H-O -H. Compared with curve Fig. 1 C a, curve Fig. 1 C b showed a similar spectra. The only differences were the band at 3400 cm^{-1} being more intense and the band at 1698 cm^{-1} showing a weaker intensity. This may be due to the abundant hydroxide groups caused by the acidification of MnO_2 and the dehydration of MnO_2 caused by concentrated acid.

The XRD patterns of MnO_2 and a-MnO_2 are shown in Fig. 1D (1D a for MnO_2, 1D b for a-MnO_2). The two samples had similar crystallographic structures. The diffraction peaks appeared at 2θ=21.8°, 37.5°, 42.1°, 49.9°, 56.2° and 66.3° matched well with the diffraction peaks of (200), (211), (301), (600) and (521) crystal planes of MnO_2 standard data (JCPDS No.80-1098) (Feng et al., 2016). When the acidification was performed in an ice water bath, the a-MnO_2 had a similar XRD pattern which indicated less damage to the original structure (Fig. 1D b). The XPS spectra of the MnO_2 and of a-MnO_2 nano-particles are presented in Supplementary material Fig. S7.

3.3. Electrochemical characteristics of the cell-based sensor

The characteristics of the fabricated RAW246.7 cell-based sensor were tested using CV, DPV, and EIS in the presence of 1.0 mM $Fe(CN)_6^{3-/4-}$. As shown in Fig. 2A and B, the voltammograms had a typical and reversible redox peak at the bare GE surface (see curve a, where the DPV current peak value was 104.6 μA). The redox current decreased slightly when the electrode was modified with a-MnO_2 (see curve b, where the DPV current peak value was 96.28 μA), owing to its weak conductivity compared with gold. The redox peak currents all decreased rapidly after the NaAlg/GO hydrogel either without or with cells immobilized on the a-MnO_2/GE (see curve c and d, where DPV current peak values were 37.24 μA and 21.17 μA, respectively). This decrease resulted from the insulation effect of complex hydrogel and cells, as the electron transfer rate of the working electrode was blocked.

The R_{et} values increased as macrophage cell numbers increased (from 5 × 10 cells/mL to 5 × 10^7 cells/mL), creating a Nyquist diagram (semi-circle) as shown in Fig. 2C. This observation was representative of a large number of immobilized cells on the electrode. When this exceeded 5 × 10^7 cells/mL, the impedance of the modified electrode became steady (not shown). Any increase in impedance was dependent on the surface's cell coverage, which was proportional to the concentration of the cells within a certain range (Fig. 2D). The R_{et} values had a linear relationship with cell concentrations from 5 × 10 to 5 ×

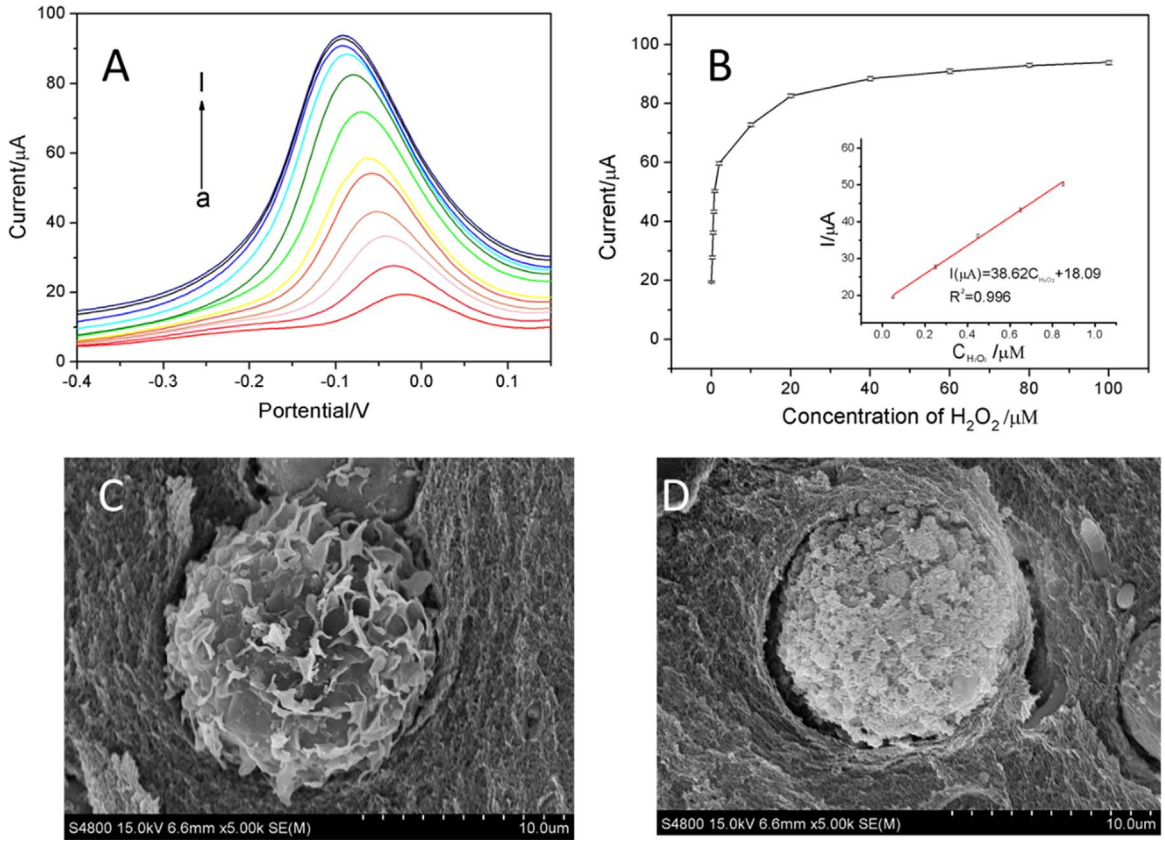

Fig. 3. (A) DPV responses of the a-MnO_2/GE for the detection of H_2O_2 released from RAW 264.7 cells induced by PMA. (a) to (l): 0 ng/mL to 100 ng/mL. (B) The corresponding calibration plots between the peak currents and H_2O_2 concentrations (from 0.05 μM to 100 μM). The morphology of (C) naive RAW264.7 cells and (D) RAW264.7 cells treated with PMA.

10^7 cells/mL, with a correlation coefficient of 0.994. When cell numbers exceeded 5 × 10^7, the impedance values were essentially unchanged. Therefore, cell number below 5 × 10^7 cells/mL was considered to be appropriate for following electrochemical analysis. In addition, the comparison of cell-based sensors and other methods is showed in Supplementary material Table. S6.

3.4. Cell-based sensor for the quantification of antioxidant activity

As essential cells in the immune system, macrophages play a key role in host protection against a wide range of foreign bodies by phagocytosis, antigen presentation, and the production of cytokines, nitrogen species (RNS), and ROS which are involved in the destruction of pathogens (Wu et al., 2011). When the cells are stimulated, respiratory bursts occur with H_2O_2 being generated as the end product. Therefore, the endogenous oxidative stress levels (antioxidant activity) in the RAW 264.7 cells induced by PMA can be evaluated by the measurement of the flux of H_2O_2 released from the cells. Thus, DPV, which suppressed the noise to improve the signal-to-noise ratio (S/N), was applied to investigate the electrochemical performance of the a-MnO_2 modified GE toward the detection of H_2O_2 released from RAW264.7 cells.

Fig. 3A displays a series of the DPV curves recorded in a 0.1 M PBS solution (pH 7.4), where the PMA concentrations varied from 0 to 100 ng/mL. A well-defined oxidation peak was observed as the dose of PMA increased. The reduction current of DPV signals rose rapidly with the increasing secretion of H_2O_2 from the cells, suggesting that the a-MnO_2 modified electrode exhibited an improved electrocatalytic oxidation activity toward H_2O_2.

Fig. 3B shows the dependence of the DPV signals (Fig. 3A) on the concentrations of H_2O_2 under the same stimulation at different PMA contents which were calculated and converted by the H_2O_2 detection ELSIA kit (Sigma-Aldrich Inc, St. Louis, MO, USA). Also the relationships among the peak current, PMA contents and H_2O_2 concentrations are shown in Supplementary material Table S7. It was found that the oxidation peaks increased gradually with increasing concentrations of H_2O_2, and a good linearity was obtained between the oxidation peak currents *Ip* and the H_2O_2 concentrations over the range from 0.05 μM to 0.85 μM, with the linear equation of *Ip* (μA) = 38.62C_{H2O2} + 18.09 and a correlation coefficient of R^2 = 0.996. The limit of detection (LOD) was calculated to be 0.02 μM according to the formula of LOD = 3 s/m, where *s* represents the standard deviation of the blank sample (n = 3) and *m* represents the slope of the relative calibration curve for H_2O_2. The sensing performance of the developed biosensor for the detection of H_2O_2 was compared with the previous reports (Supplementary material Table S5). Based on the comparison listed in Table S5, the cell-based sensor had an excellent detection performance as well as being a more convenient operational process. In addition, the comparison between the Cell/NaAlg/GO/a-MnO_2/GE and Cell/NaAlg/GO/MnO_2/GE for the analysis of H_2O_2 is shown in Supplementary material Fig. S6.

SEM images of RAW264.7 cells showed long microvilli and emitting filamentous pseudopods on the surface of the macrophage plasma membrane (Fig. 3C). However, microvilli on the plasma membrane showed spot-like distributions which became scarce in some locations and most of the membranes became smooth when the H_2O_2 was released from RAW264.7 cells sensitized by PMA (Fig. 3D). This may explain the results that the DPV peak current increased as the intracellular oxidative stress level decreased.

The reproducibility and stability of a-MnO_2/GC electrode for determining the oxidative stress level in RAW264.7 cells was evaluated by detecting H_2O_2 (0.85 μM) in PBS solution. The results revealed that the modified electrode gave reproducible results with a relative standard deviation (R.S.D) of 5% for 10 parallel measurements. After

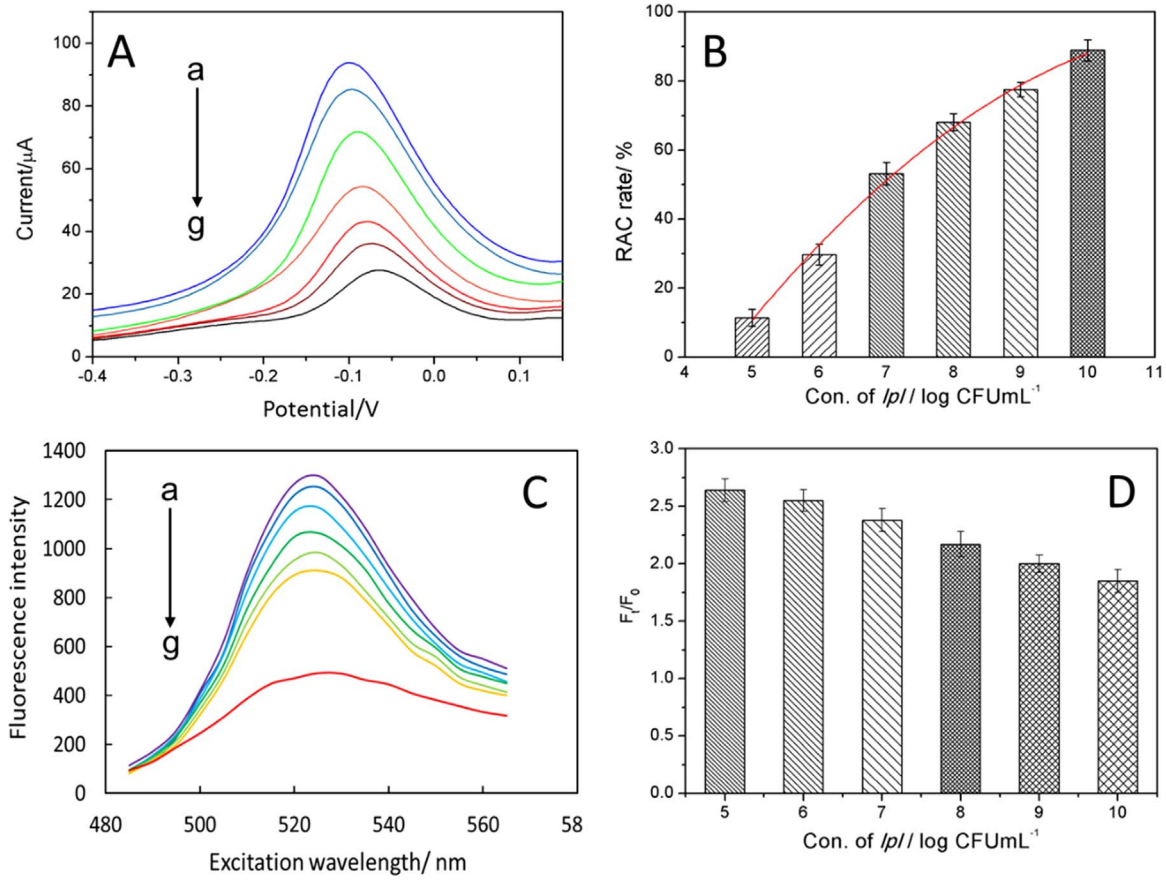

Fig. 4. (A) The oxidation peak current of the RAW264.7 cell-based senor incubated with different concentrations of *L. plantarum* extracts, a for positive control (cells without *L. plantarum* incubation), b to g: 10^5, 10^6, 10^7, 10^8, 10^9, 10^{10} CFU/mL, cells in all these groups are treated with 100 mg/mL PMA. (B) Relative antioxidant capacity of different concentrations of *L. plantarum* extracts from 10^5 to 10^{10} CFU/mL. (C) Fluorescent detection of ROS in RAW246.7 cells incubated with different concentrations of *L. plantarum* extracts, g for negative control (cells without PMA stimulation), a to f: 10^5, 10^6, 10^7, 10^8, 10^9, 10^{10} CFU/mL, cells in all these groups are treated with 100 mg/mL PMA. (D) The relative fluorescence intensity rate (F_t/F_0) of different concentrations of *L. plantarum* extracts from 10^5 to 10^{10} CFU/mL.

the modified electrode had been stored at room temperature for 10 days, only a small decrease in the response current (about 3.2%) was observed. These results demonstrate that the electrode exhibits satisfactory reproducibility and stability, indicating that the developed cell sensor is suitable for the practical analysis of antioxidant ability in authentic samples.

3.5. Application of the cell-based sensor for evaluating the antioxidant capacity of L. plantarum

In order to effectively evaluate the antioxidant ability of *L. plantarum* strains, the appropriate amount of PMA should be selected to ensure the maximum oxidative stress reaction occurring in RAW264.7 cells on the a-MnO_2/GC electrode. Hence, according to the H_2O_2 detection results in Fig. 3, the value of peak current (I_P) increased sharply with the secretion of the H_2O_2 with no obvious increase of the I_P value being observed when the concentration of H_2O_2 was higher than 100 μM. Therefore, 100 μM of H_2O_2, which corresponded to 100 ng/mL of PMA stimulation, was selected as the optimum concentration for evaluating the antioxidant ability of *L. plantarum* strains.

Then the antioxidant capacity of the different extracts (derived from different cell numbers) of *L. plantarum* strains was studied by DPV analysis (Fig. 4A). It was noted that the values of peak current *Ip* decreased with extracts derived from higher cell numbers of *L. plantarum* compared with the positive control (cells incubated without *L. plantarum* extracts). This can be explained by its inhibitory effect on the release of H_2O_2. Here, the antioxidant ability of the *L. plantarum* strains was expressed as the value of relative antioxidant capacity (RAC) which is demonstrated by the following algorithm:

$$\text{Relative antioxidant capacity(RAC)} = \frac{I_0 - I_S}{I_0 - I} \times 100\%$$

Where I_0 is the DPV peak current with a stimulation of 100 ng/mL PMA, I_S is the DPV peak current in the presence of *L. plantarum* extracts, and I is the peak current without the PMA sensitized and *L. plantarum* extract incubation.

The relationship between the RAC rate and the concentration of *L. plantarum* extracts is shown in Fig. 4B. It can be observed that the RAC rate increased dramatically with increasing concentrations of *L. plantarum* extracts ranging from 10^5 to 10^{10} CFU/mL.

The antioxidant capacities of *L. plantarum* extracts derived from a range of cell numbers were investigated following stimulation with PMA (100 mg/L). The RAC rates of 10^5, 10^6, 10^7, 10^8, 10^9 and 10^{10} CFU/mL of *L. plantarum* extracts were calculated as 11.44%, 29.7%, 53.14%, 68.08%, 77.55%, and 88.94%, respectively. The results showed that different concentrations of *L. plantarum* extracts had various antioxidant capacities and were dose dependent, showing the highest antioxidant activity (88.94%) with extracts derived from 10^{10} CFU/mL. These suggest that extracts derived from higher cell numbers of *L. plantarum* strains have greater antioxidant capacity, which is consistent with the report of Jakubczak et al. (2012). In order to verify the validity of electrochemical detection method, ROS production in RAW246.7 cells incubated with extracts from different cell numbers of *L. plantarum* extracts was stimulated using the same concentration of PMA as used previously. Since the intracellular

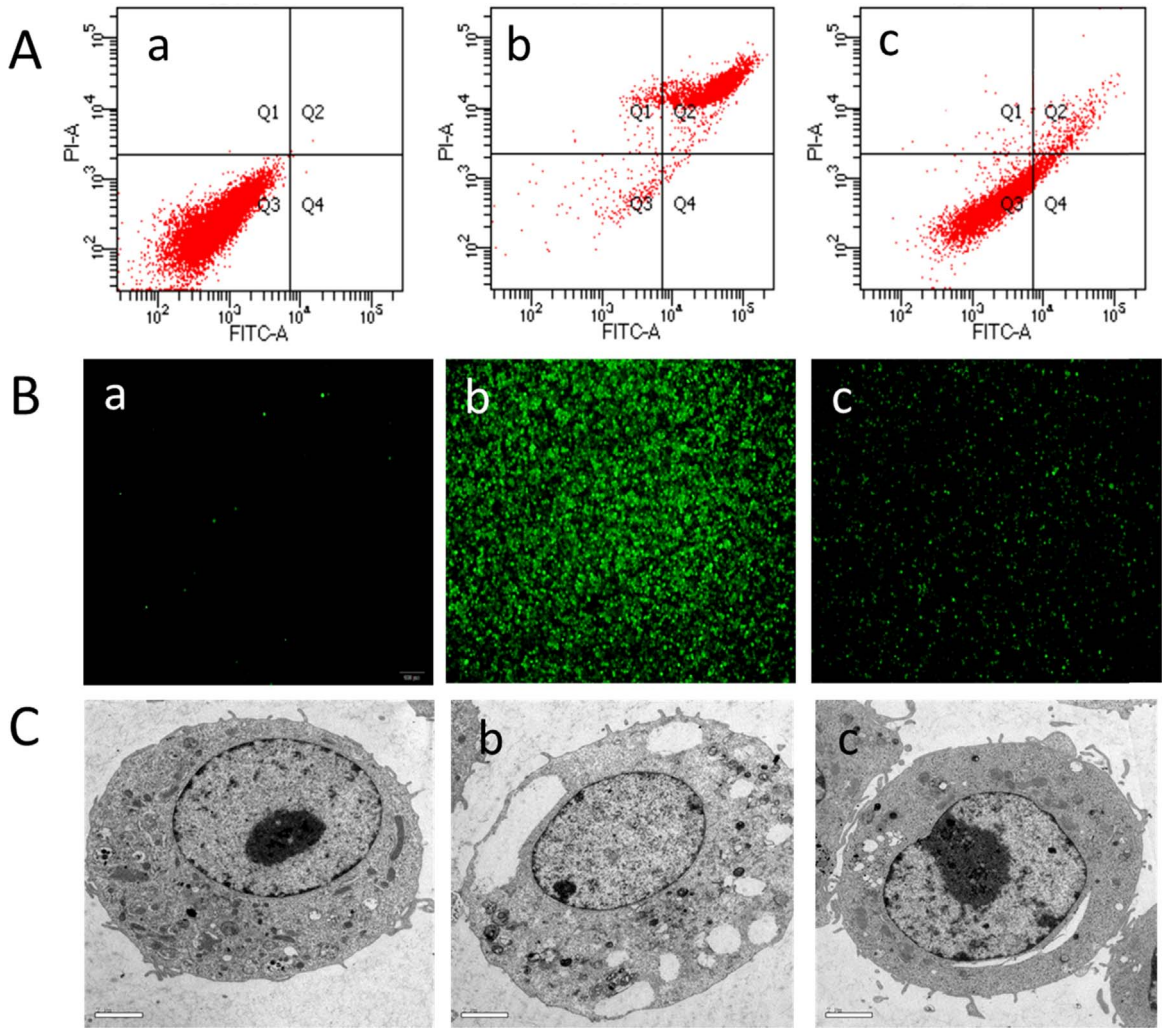

Fig. 5. Antioxidant effect of *L. plantarum* extracts on the RAW264.7 cells obtained by the traditional biological assay. (A) FACS analysis of apoptosis in RAW264.7 cells with different treatments. (B) Fluorescent measurement of ROS in RAW264.7 cells with different treatments. (C) Transmission electron micrograph of RAW264.7 cells with different treatments. Notes: a for control, b for RAW264.7 cells in response to 100 μM H_2O_2 and c for RAW264.7 cells incubated with 10^{10} CFU/mL of *L. plantarum* extracts before treated with 100 μM H_2O_2.

generation of ROS is correlated with oxidative stress levels in the cells, it is reflected in the form of cellular fluorescence. Therefore, as shown in Fig. 4C, the intracellular fluorescence intensity significantly decreased with the increase of *L. plantarum* extracts (from 10^5 to 10^{10} CFU/mL) compared with the control group, indicating that oxidative stress levels in cells were effectively inhibited through biochemical effects of *L. plantarum* strains. A histogram of the relationship between the contents of *L. plantarum* extracts and the relative fluorescence intensity rates F_t/F_0 is shown in Fig. 4D, where F_t is defined as the fluorescence intensity of sample at the given time point, and F_0 as the fluorescence intensity of control. The changes of fluorescence intensity, quantified by the ratio of F_t/F_0, clearly showed that the fluorescence intensities were followed with a similar trend to that of the DPV. The fluorescence ratios of 10^5, 10^6, 10^7, 10^8, 10^9 and 10^{10} CFU/mL of L. *plantarum* extracts were calculated as 2.64, 2.55, 2.38, 2.17, 2.00, and 1.85, respectively. The 10^{10} CFU/mL of L. *plantarum* extracts had the lowest fluorescence ratio (1.85), implying that these extracts had the highest antioxidant capacity.

Therefore, these data are in agreement with those results based on the cell-based electrochemical method, indicating that the proposed cell-based biosensor has potential use for the determination and evaluation of total antioxidant capacities in natural and synthetic antioxidants. In addition, the comparison of RAC rate between *L. plantarum*, VC, VE and TP is shown in Supplementary material Fig. S5.

3.6. Effect of L. plantarum extracts on intracellular oxidative stress

To estimate the antioxidant effects of *L. plantarum* strains and to verify the detection results of electrochemical method, *L. plantarum* extracts obtained from 10^{10} CFU/mL were used for cell viability assay, intracellular ROS detection, and TEM observation (Fig. 5). Because ROS species can specifically induce apoptosis in neutrophils and macrophages, we conducted apoptosis analysis by flow cytometry using the 100 μM H_2O_2 sensitized RAW264.7 cells in the presence or absence of *L. plantarum* extracts. They were incubated with either Annexin V-FITC or PI as markers for apoptosis and necrosis, respectively (Fig. 5A). There were clearly low rates of early apoptosis (4.1 ± 0.04 *vs.* $5.3 \pm 0.06\%$), late apoptosis ($6.1 \pm 0.03\%$ *vs.* $90.6 \pm 0.05\%$) and necrosis (0.6 ± 0.05 *vs.* $1.7 \pm 0.04\%$) as shown in Fig. 5A (c and b). About 97.6% of the total cells were apoptotic in response to 100 μM H_2O_2, but no significant apoptosis (only 10.8% of the total cells) was observed in the presence of extracts from *L. plantarum* at 10^{10} CFU/mL. Therefore, it is evident that *L. plantarum* strains have a powerful ability to inhibit cell apoptosis. This implies that there is potential for various applications for its antioxidant capacity in living organisms.

Intracellular ROS production has long been recognized as a significant factor in oxidative stress of cell, and is also an important messenger associated with macrophage activation. We investigated the effects of *L. plantarum* extracts on calcium signaling in RAW264.7

cells using appropriate fluorescent molecular probes. The stimulation of cells with 100 μM H_2O_2 induced a rapid emergence of green fluorescence in the cells and an increase in fluorescence intensity (Fig. 5B b) compared with the control (Fig. 5B a), indicating a robust rise in oxidative stress levels in the cytoplasm. On the contrary, the green fluorescence dramatically decreased when the RAW264.7 cells were incubated with the extracts derived from 10^{10} CFU/mL of *L. plantarum*, verifying the strong antioxidant characteristic of *L. plantarum* (Fig. 5B c).

The composition of cell cytoplasm was greatly influenced by the extent of intracellular oxidative stress. Fig. 5C shows the TEM images of RAW264.7 cells incubated with or without *L. plantarum* extracts before being sensitized with H_2O_2. Nuclei and cell plasma projections were clearly visible in the TEM image of the control group (Fig. 5C a). However, following the exposure of RAW 264.7 cells to 100 μM H_2O_2, there was evidence of the dilation of endoplasmic reticulum, the swelling of mitochondria, the dissolution of nucleus and a large number of vesicles in the cell cytoplasm (Fig. 5C b), indicating that there was a higher level of oxidative stress in the cells. However, when RAW264.7 cells were incubated with 10^{10} CFU/mL of *L. plantarum* extract, they exhibited an obvious restoration of cell structure, as indicated by the reduction in vesicles numbers, the contraction of endoplasmic reticulum, as well as the recovery of the endosome membrane (Fig. 5C c). Again, this clearly shows that, *L. plantarum* has a strong ability to reduce oxidative stress levels in living cells. In the Supplementary material section, it was shown that lipid oxidation was reduced in RAW264.7 cells. In addition, the changes in total intracellular SOD activity (using the WST-8 assay) provided further evidence of the antioxidant effectiveness of extracts from *L. plantarum*. See Supplementary material section 2 (Fig. S2, Table S2 and S3) and Section 3 (Fig. S3 and Table S4).

4. Conclusion

In this study, a highly sensitive and inexpensive RAW264.7 cell-based biosensor was developed by immobilizing living RAW264.7 cells on an a-MnO_2 modified GE for quantifying the antioxidant capacity of *L. plantarum* strains. The method was developed in effort to exploit a new technology for evaluating antioxidant properties of various antioxidants, based on the measurement of intracellular hydrogen peroxide levels. Alginate/graphene oxide hydrogels were synthesized, characterized, and encapsulated around RAW264.7 cells giving a good correlation with cell concentrations from 5×10^1 to 5×10^7 cells/mL.

The proposed cell-based electrochemical method represents substantial potential advantages over conventional assays. Using PMA, a well-established ROS stimulator, induced a robust and dose-dependent DPV signal. Peak current changes indicated the generation of H_2O_2 from RAW264.7 cells, and the intracellular oxidative stress levels were monitored in real-time by electrochemical detection. The I_p values were proportional to H_2O_2 concentrations ranging from 0.05 to 0.85 μM with a correlation coefficient of 0.996 at a detection limit of 0.02 μM. The method was then used to determine the effectiveness of cell-free extracts of *L. plantarum* NJAU-01 isolated from traditional Chinese dry-cured ham for their *in vitro* antioxidant capacity. The detection signal intensity of I_p values decreased as intracellular cell-free extracts of *L. plantarum* contents increased, indicating that *L. plantarum* strains, at a dose of 10^{10} CFU/mL, had the highest antioxidant activity with RAC rates of 88.94%. Moreover, ROS fluorescence detection and cell viability assay were employed to verify the robustness of cell-based sensor. The results suggest that the proposed electrochemical cell-based sensor can accurately evaluate the antioxidant capacity of extracts of *L. plantarum* on RAW264.7 cells. The proposed method is simple, rapid and inexpensive, and allows for convenient electrode renewal. The RSD of the detection results was lower than 5%, indicating that the cell sensor had good reproducibility and stability. The new method can be considered as a real alternative to the present involved and expensive methods of antioxidant activity detection.

Acknowledgments

This work has been supported by the National Key Research and Development Program of China of the Thirteenth Five Plan (2016YFD0400703), National Natural Science Foundation of China (No. 31571853, 31601535, 31371792), Natural Science Foundation of Jiangsu Province (No. BK20160459) and the Priority Academic Program Development of Jiangsu Higher Education Institutions (No. 16KJB550008).

Appendix A. Supporting information

Supplementary data associated with this article can be found in the online version at doi:10.1016/j.bios.2017.08.037.

References

Ahmad, H., Ahmad, S., Shah, S.A.A., Latif, A., Ali, M., Khan, F.A., Tahir, M.N., Shaheen, F., Wadood, A., Ahmad, M., 2017. Bioorgan. Med. Chem. 25 (13), 3368–3376.
Andlauer, W., Heritier, J., 2011. Food Chem. 125, 1517–1520.
Bai, W., Zhang, X., Zhang, S., Sheng, Q., Zheng, J., 2017. Sens. Actuators B-Chem. 242, 718–727.
Blois, M.S., 1958. Nature 181, 1199–1200.
Bordonaba, J.G., Terry, L.A., 2012. Talanta 90, 38–45.
Cata, A., Stefanut, M.N., Pop, R., Tanasie, C., Mosoarca, C., Zamfir, A.D., 2016. Croat. Chem. Acta 89, 37–48.
Chakraborty, S., Raj, C.R., 2009. Biosens. Bioelectron. 24, 3264–3268.
Das, P., Das, M., Chinnadayyala, S.R., Singha, I.M., Goswami, P., 2016. Biosens. Bioelectron. 79, 386–397.
Dickinson, B.C., Chang, C.J., 2011. Nat. Chem. Biol. 7, 504–511.
Ervin, E.M., Kariuki, J.K., 2014. Int. J. Electrochem. Sci. 9, 6235–6245.
Feng, L., Wang, R., Shi, Y., Wang, H., Yang, J., Zhu, J., Chen, Y., Yuan, N., 2016. Int. J. Electrochem. Sci. 11, 5962–5972.
Gao, F., Zheng, D., Tanaka, H., Zhan, F., Yuan, X., Gao, F., Wang, Q., 2015. Mater. Sci. Eng.: C 57, 279–287.
Gimeno, P., Bousquet, C., Lassu, N., Maggio, A.-F., Civade, C., Brenier, C., Lempereur, L., 2015. J. Pharm. Biomed. 107, 386–393.
Ignatov, S., Shishniashvili, D., Ge, B., Scheller, F.W., Lisdat, F., 2002. Biosens. Bioelectron. 17, 191–199.
Jakubczak, A., Stachelska, M.A., Swislocka, R., Lewandowski, W., 2012. Pol. J. Natur. Sc. 27, 81–92.
Jiang, D., Feng, D., Jiang, H., Yuan, L., Yongqi, Y., Xu, X., Fang, W., 2017. Biosens. Bioelectron. 90, 436–442.
Jiang, D., Jiang, H., Ji, J., Sun, X., Qian, H., Zhang, G., Tang, L., 2014. J. Agr. Food Chem. 62, 6473–6480.
Kamel, A.H., Moreira, F.T., Delerue-Matos, C., Sales, M.G.F., 2008. Biosens. Bioelectron. 24, 591–599.
Lee, S.M., Han, N., Lee, R., Choi, I.H., Park, Y.B., Shin, J.S., Yoo, K.H., 2016. Biosens. Bioelectron. 77, 56–61.
Li, S., Zhao, Y., Zhang, L., Zhang, X., Huang, L., Li, D., Niu, C., Yang, Z., Wang, Q., 2012. Food Chem. 135, 1914–1919.
Luo, D., Fang, B., 2008. Carbohyd. Polym. 72, 376–381.
Ou, B., Hampsch-Woodill, M., Prior, R.L., 2001. J. Agr. Food Chem. 49, 4619–4626.
Pazourek, J., Gajdošová, D., Spanilá, M., Farková, M., Novotná, K., Havel, J., 2005. J. Chromatogr. A 1081, 48–54.
Pi, J., Jin, H., Jiang, J., Yang, F., Cai, H., Yang, P., Cai, J., Chen, Z.W., 2017. Pharmacol. Res. 119, 479–489.
Prenesti, E., Berto, S., Daniele, P.G., Toso, S., 2007. Food Chem. 100, 433–438.
Qiao, J., Liu, Z., Tian, Y., Wu, M., Niu, Z., 2015. Chem. Commun. 51, 3641–3644.
Reybier, K., Ribaut, C., Coste, A., Launay, J., Fabre, P.L., Nepveu, F., 2010. Biosens. Bioelectron. 25, 2566–2572.
Rider, T.H., Petrovick, M.S., Nargi, F.E., Harper, J.D., Schwoebel, E.D., Mathews, R.H., Blanchard, D.J., Bortolin, L.T., Young, A.M., Chen, J., 2003. Science 301, 213–215.
Romero, M.P.R., Brito, R.E., Palma, A., Montoya, M.R., Mellado, J.M.R., Rodriguez-Amaroa, R., 2017. J. Electrochem. Soc. 164, B97–B102.
Taniguchi, A., 2010. Biomaterials 31, 5911–5915.
Tufan, A.N., Baki, S., Guclu, K., Ozyurek, M., Apak, R., 2014. J. Agr. Food Chem. 62, 7111–7117.
Wang, L., Zhang, Y., Cheng, C., Liu, X., Jiang, H., Wang, X., 2015. ACS Appl. Mater. Interfaces 7, 18441–18449.
Wang, X., Jiao, C., Yu, Z., 2014. Sens. Actuators B-Chem. 192, 628–633.
Wang, X., Zhu, P., Pi, F., Jiang, H., Shao, J., Zhang, Y., Sun, X., 2016. Biosens. Bioelectron. 81, 349–357.
Wu, P., Cai, Z., Chen, J., Zhang, H., Cai, C., 2011. Biosens. Bioelectron. 26, 4012–4017.
Xu, B., Ye, M.-L., Yu, Y.-X., Zhang, W.-D., 2010. Anal. Chim. Acta 674, 20–26.
Zhang, D., Yin, R.Y., Liu, Y.X., Li, X., Zhou, F., Ji, B.P., 2015. Food Anal. Methods 8, 2218–2227.
Zhao, Y., Huo, D., Bao, J., Yang, M., Chen, M., Hou, J., Fa, H., Hou, C., 2017. Sens. Actuators B-Chem. 244, 1037–1044.